LLNL-PROC-414495

Improving Earthquake-Explosion Discrimination Using Attenuation Models of the Crust and Upper Mantle

M. E. Pasyanos, W. R. Walter, E. M. Matzel, A. J. Rodgers, S. R. Ford, R. Gok, and J. J. Sweeney

July 8, 2009

2009 Monitoring Research Review
Tucson, AZ, United States
September 21, 2009 through September 23, 2009

IMPROVING EARTHQUAKE-EXPLOSION DISCRIMINATION USING ATTENUATION MODELS OF THE CRUST AND UPPER MANTLE

Michael E. Pasyanos, William R. Walter, Eric M. Matzel, Arthur J. Rodgers, Sean R. Ford, Rengin Gök, and Jerry J. Sweeney

Lawrence Livermore National Laboratory
Sponsored by National Nuclear Security Administration
Contract No. DE-AC52-07NA27344

ABSTRACT

In the past year, we have made significant progress on developing and calibrating methodologies to improve earthquake-explosion discrimination using high-frequency regional P/S amplitude ratios. Closely-spaced earthquakes and explosions generally discriminate easily using this method, as demonstrated by recordings of explosions from test sites around the world. In relatively simple geophysical regions such as the continental parts of the Yellow Sea and Korean Peninsula (YSKP) we have successfully used a 1-D Magnitude and Distance Amplitude Correction methodology (1-D MDAC) to extend the regional P/S technique over large areas. However in tectonically complex regions such as the Middle East, or the mixed oceanic-continental paths for the YSKP the lateral variations in amplitudes are not well predicted by 1-D corrections and 1-D MDAC P/S discrimination over broad areas can perform poorly.

We have developed a new technique to map 2-D attenuation structure in the crust and upper mantle. We retain the MDAC source model and geometrical spreading formulation and use the amplitudes of the four primary regional phases (Pn, Pg, Sn, Lg), to develop a simultaneous multi-phase approach to determine the P-wave and S-wave attenuation of the lithosphere. The methodology allows solving for attenuation structure in different depth layers. Here we show results for the P and S-wave attenuation in crust and upper mantle layers.

When applied to the Middle East, we find variations in the attenuation quality factor Q that are consistent with the complex tectonics of the region. For example, provinces along the tectonically-active Tethys collision zone (e.g. Turkish Plateau, Zagros) have high attenuation in both the crust and upper mantle, while the stable outlying regions like the Indian Shield generally have low attenuation. In the Arabian Shield, however, we find that the low attenuation in this Precambrian crust is underlain by a high-attenuation upper mantle similar to the nearby Red Sea Rift. Applying this 2-D MDAC methodology with the new attenuation models can significantly improve earthquake-explosion discrimination using regional P/S amplitude ratios. We demonstrate applications of this technique, including a study at station NIL (Nilore, Pakistan) using broad area earthquakes and the 1998 Indian nuclear explosion using a number of regional amplitude ratio discriminants. We are currently applying the technique in the YSKP region as well.

OBJECTIVE

Our objective is to develop and calibrate methodologies to improve earthquake-explosion discrimination using high-frequency regional P/S amplitude ratios. It has been demonstrated that closely-spaced earthquakes and explosions generally discriminate easily using this method. For example, the green and red waveforms shown in Figure 1 are a closely-located earthquake and explosion pair recorded at the same station and using the same filtering. The explosion (shown in red) has a much larger ratio of P-wave energy to S-wave energy than the nearby earthquake (shown in green). Lateral variations in attenuation, however, can produce large changes in the amplitudes of regional phases, which can degrade the performance of these discriminants over the broad region. In Figure 1, for instance, the cyan waveform shows an explosion-like earthquake (high P-to-S ratio) located far from the explosion shown. In the past, we have shown that the Magnitude and Distance Amplitude Correction (MDAC) methodology (Walter and Taylor, 2001) can account for simple 1-D attenuation and geometrical spreading corrections, as well as site effects. In complex regions like the Middle East, however, 1-D path corrections are a poor approximation, and we need to develop 2-D path corrections that can account for the structure. Our approach is to calibrate the attenuation structure, and to use this model to better separate the populations of earthquakes and explosions.

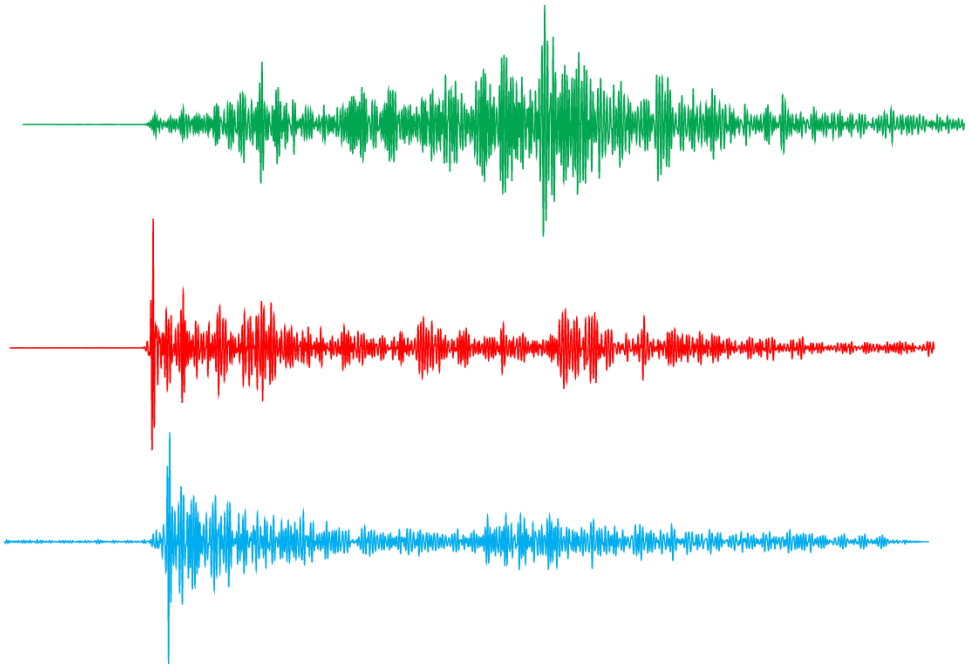

Figure 1. Waveforms of two earthquakes (shown in green and cyan) and the 1998 Indian nuclear explosion (shown in red) recorded at station NIL and filtered between 1-2 Hz. (figure from Pasyanos and Walter, 2009).

RESEARCH ACCOMPLISHED

We have made significant progress on calibrations since the last seismic review (Walter et al., 2008). First, we have developed a four-phase amplitude tomography which allows us to determine a consistent set of attenuation, site, and source corrections for the primary regional phases of Pn, Pg, Sn, and Lg. Secondly, we have demonstrated that we can use the attenuation model to correct phase amplitudes and improve high-frequency P/S discriminants. While we primarily discuss results from the Middle East region, we are currently applying the technique in the Yellow Sea – Korean Peninsula (YSKP) region as well.

Amplitude Tomography

Recent work has focused on the attenuation of regional phases in the Middle East and vicinity and has been the subject of several recent publications (Pasyanos et al., 2009a, 2009b). Like most amplitude tomography, we assume

that the observed amplitudes are a product of four terms: the source term S, the geometrical-spreading term G, the attenuation term B, and the site term P.

$$A_{ij} = S_i \; G_{ij} \; B_{ij} \; P_j \qquad (1)$$

where i is an event index and j is a station index.

Our methodology, employed in Pasyanos et al. (2009a) for Lg, uses an MDAC source model (Walter and Taylor, 2001), which more explicitly defines the source expression in terms of an earthquake source model formulated in terms of the seismic moment. One of the advantages of this approach is to easily estimate the predicted Lg amplitudes for an event of any given location and size. We assume a geometrical spreading and provide parameters that relate the initial source term to the moment. Using amplitudes for about 6000 Lg paths, we then initialize the attenuation, site, and source terms and solve for all three sets of parameters in several different frequency bands from 0.5 – 10 Hz.

In a subsequent paper (Pasyanos et al., 2009b), we applied the technique to simultaneously invert 1-2 Hz amplitudes of Pn, Pg, Sn and Lg to produce P-wave and S-wave attenuation models of the crust and upper mantle. The attenuation is modeled as P-wave and S-wave attenuation surfaces for the crust, and a similar set for the upper mantle. We can use all of the phase amplitudes together by using the appropriate (source, geometrical-spreading, site, and attenuation) terms for each phase. For example, the source terms of the P-waves and S-waves are different, and path attenuation is calculated by raypaths appropriate for the particular phase. Inverting all of the phases simultaneously (in this case, amplitudes for about 12,000 paths; see Figure 2) allows us to determine consistent attenuation, site, and source terms for all phases, and eliminates non-physical inconsistencies among them.

The terms shown in equation (1) are specified as follows. The source term S is based on the MDAC source model and for P-waves and S-waves are specified as:

$$S^P = F^P M_o/(1+(\omega/\omega^P_c)^2) \qquad (2)$$
$$S^S = F^S M_o/(1+(\omega/\omega^S_c)^2) \qquad (3)$$

where M_o is the seismic moment, the $F M_o$ term is the long-period radiated energy, ω is angular frequency, ω_c is the corner frequency and P and S superscripts indicate P-wave and S-waves. We use the geometrical spreading form of Street et al. (1975):

$$G(R) = \begin{cases} 1/R & \text{if } R < R_o \\ (1/R_o)(R_o/R)^n & \text{if } R >= R_o \end{cases} \qquad (4)$$

where R is distance, R_o is the critical distance, and n is the spreading variable. The values of R_o and n depend on the phase. The attenuation term B is specified as:

$$B_{ij} = \exp\left[-\frac{\omega}{2}\sum_{k=1}^{nlayers}\frac{r_k}{Q_k v_k}\right] \qquad (5)$$

where r is distance, Q is the attenuation quality factor, and v is the velocity. The layers sampled depend on the model and phase. We simplify the problem by specifying the velocity structure as a layer over a half-space. This parameterization has the crustal phases Pg and Lg sampling the crustal layer only, while the mantle phases Pn and Sn sample both the upper mantle layer and the crustal layer under the source and station. It is possible to expand the number of layers further in the future as regional phase coverage improves. The last term, the site term P, is simply a multiplicative factor applied for the station and phase.

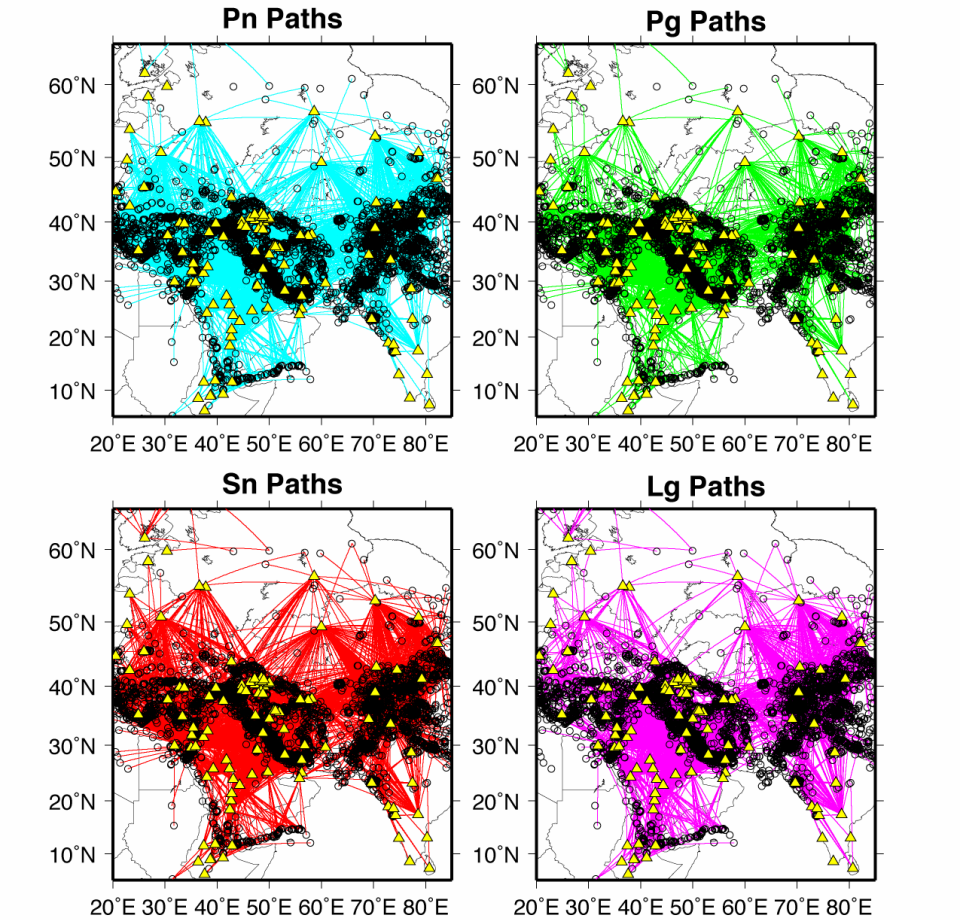

Figure 2. Path map of Pn, Pg, Sn, and Lg attenuation measurements in our study area. Stations are shown as yellow triangles, events as black circles, and paths as cyan lines (Pn), green lines (Pg), red lines (Sn), and magenta lines (Lg). Figure from Pasyanos et al. (2009b).

We use tomography to determine the P-wave and S-wave attenuation of the crust and upper mantle, along with corresponding site and event terms. We find variations in the attenuation quality factor Q across the Middle East that are consistent with the complex tectonics of the region. For example, in Figure 3 we find that provinces along the tectonically-active Tethys collision zone (e.g. Turkish Plateau, Zagros) have high attenuation in both the crust and upper mantle, while the stable outlying regions like the Indian Shield generally have low attenuation. While variations in crust and upper mantle attenuation are often similar, they are decoupled. In the Arabian Shield, for instance, we find that the low attenuation in this Precambrian crust is underlain by a high-attenuation upper mantle similar to the nearby Red Sea Rift. This is appropriate given the tectonics of the region indicated by the volcanics and velocity studies, which find slow, hot material in the crust along the rift, but spread out under the Arabian Shield in the mantle (e.g. Camp and Roobol, 1992).

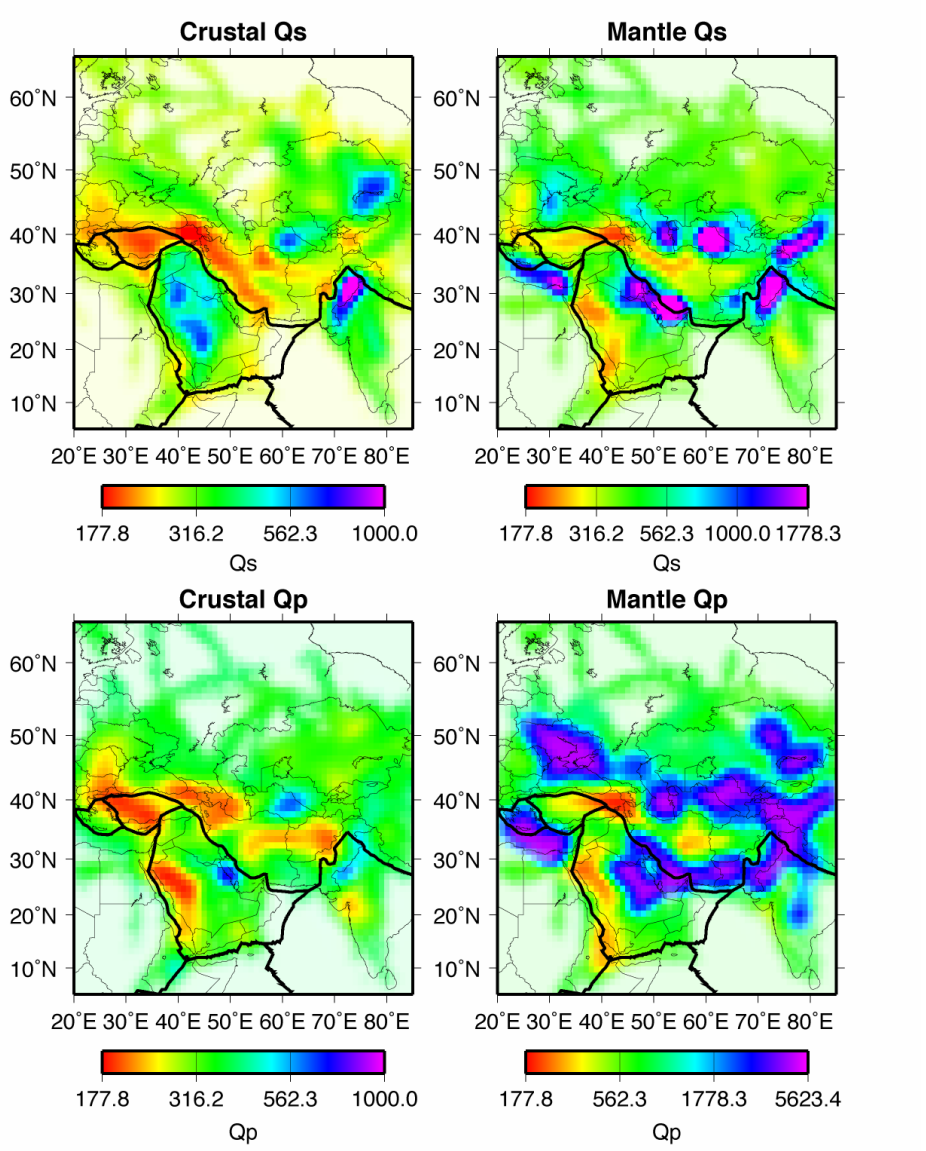

Figure 3. Maps of attenuation quality factor Q for shear-wave attenuation in the crust (crustal Qs), shear-wav attenuation in the mantle (mantle Qs), compressional-wave attenuation in the crust (crustal Qp), and compressional-wave attenuation in the mantle (mantle Qp). Dark lines indicate plate boundaries from Bird (2003). Figure from Pasyanos et al. (2009b).

Discrimination

Applying corrections with the new attenuation models can significantly improve earthquake-explosion discrimination using regional P/S amplitude ratios. We demonstrate applications of this technique, including a study at station NIL (Nilore, Pakistan) using broad area earthquakes and the 1998 Indian nuclear explosion using a number of regional amplitude ratio discriminants, as presented in Pasyanos and Walter (2009).

P/S discriminants are expressed as the ratio between the P-wave amplitude (A^P) and the S-wave amplitude (A^S) and, because of the large variations, are usually plotted on a log scale. We examine the ratio of Pn amplitudes to Lg amplitudes in the 1-2 Hz passband recorded at station NIL in Nilore, Pakistan. Figure 4 shows the ratio of the raw amplitudes as a function of distance and in map view. Besides the clear trend with distance (a result of the differing geometrical spreading and attenuation of the two phases), there is very large scatter in the earthquake population,

which is due to a combination of factors, among them variations in path attenuation. Notice as well the Indian nuclear explosion of 11 May 1998 (plotted as a red star) falls within the scatter of the earthquakes, and the explosion cannot be reliably discriminated. Notice as well the large colored circles on the left-hand plot which correspond to the waveforms shown in Figure 1. In terms of the raw amplitude ratio, we see that the cyan circle is actually more explosion-like than the actual explosion.

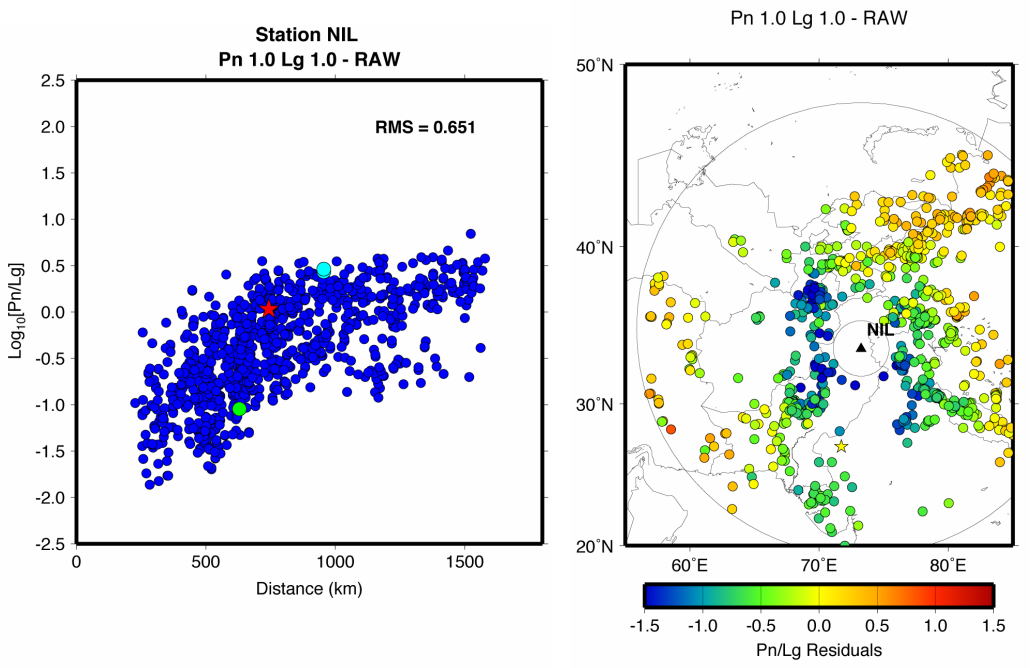

Figure 4. Pn/Lg discriminant at 1-2 Hz frequency recorded at station NIL showing raw data. Left panel shows discriminant as a function of distance. The three waveforms shown in Figure 1 are indicated by their corresponding color. Right panel shows map view with symbols colored by the P/S ratio. Left panel from Pasyanos and Walter (2009).

In order to correct the phase ratio for path and source effects, we adjust the individual amplitudes assuming an earthquake source. We then form our discriminant using the ratio of the corrected amplitudes. This is a division of the amplitudes or a subtraction in log-space:

$$\text{discriminant} = \log\left[\frac{(A^P/A_0^P)}{(A^S/A_0^S)}\right] = \log\left[\frac{A^P}{A^S}\right] - \log\left[\frac{A_0^P}{A_0^S}\right] \qquad (6)$$

where A_0 are the amplitude predictions for an earthquake of that phase and size. As a result, the corrected discriminant should now have a value around 0 (P/S ratio of 1) for earthquakes. We input a best estimate of the earthquake size by using a moment magnitude, if available, or otherwise estimating Mw using other magnitude estimates.

The discriminant using corrected amplitudes is shown in Figure 5. The attenuation and geometrical spreading have minimized the trend with distance, the scattering of the earthquake population is reduced, and most importantly, the explosion separates cleanly from the earthquakes. Lg paths traversing regions of high crustal Q (e.g. to the south of NIL) will be normalized by high Lg amplitudes and hence have a higher P/S ratio. Those traversing regions of low crustal Q (e.g. to the north) will be normalized by low Lg amplitudes and have a lower P/S ratio.

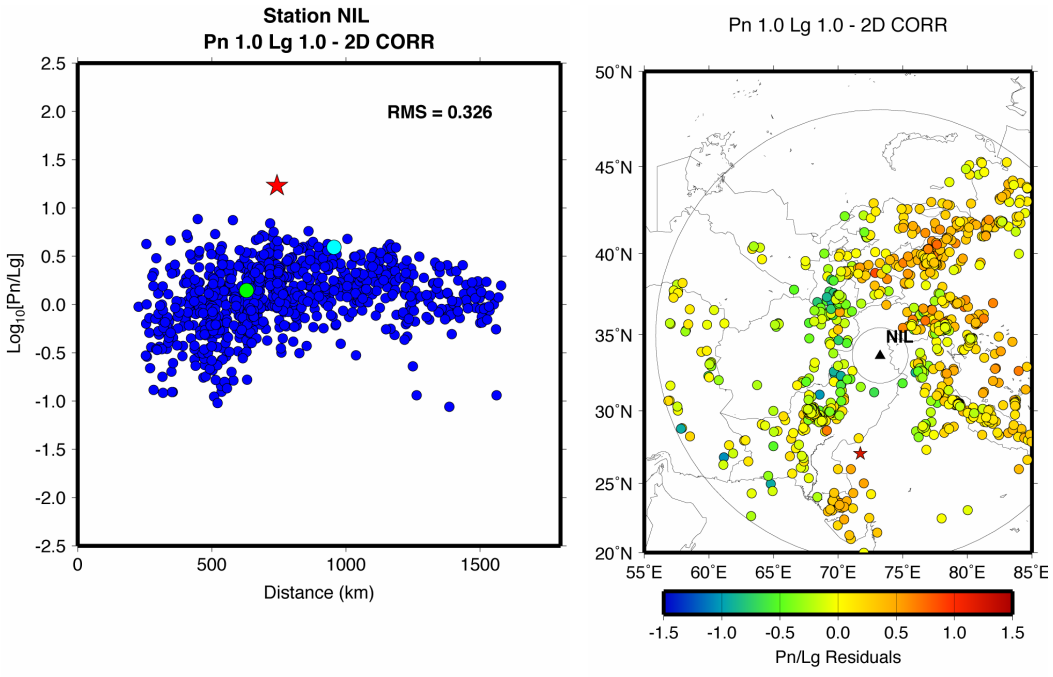

Figure 5. Pn/Lg discriminant at 1-2 Hz frequency recorded at station NIL showing data with attenuation corrections. Left panel shows discriminant as a function of distance. The three waveforms shown in Figure 1 are indicated by their corresponding color. Right panel shows map view with symbols colored by the P/S ratio. Figure from Pasyanos and Walter (2009).

It is important to note that in many areas where the lateral attenuation variations are low, we could correct the trends in distance and magnitude with a 1D correction. In this region, however, simply removing the trend would reduce the RMS of the earthquake population from 0.65 to 0.62 log-units, but the explosion would not separate from the earthquakes as the corrections would be the same for a given distance. Where lateral variations in attenuation are high, only 2D corrections can start to account for the large observed amplitude variations. After the attenuation corrections are applied, the RMS of the earthquake amplitude residuals reduces further to 0.326.

We also look at the discrimination using a number of other combinations of regional P/S amplitudes, including Pn/Sn and Pg/Lg. The results are shown in Figure 6. Like the Pn/Lg discriminant, in the raw data these discriminants did not cleanly separate the explosion from the earthquake population until the attenuation correction was applied. We can see that the attenuation model of the crust and upper mantle seems to be predictive for all major regional phases (Pn, Pg, Sn, Lg), which are all represented in various combinations in the three discriminants (Pn/Lg, Pn/Sn, Pg/Lg).

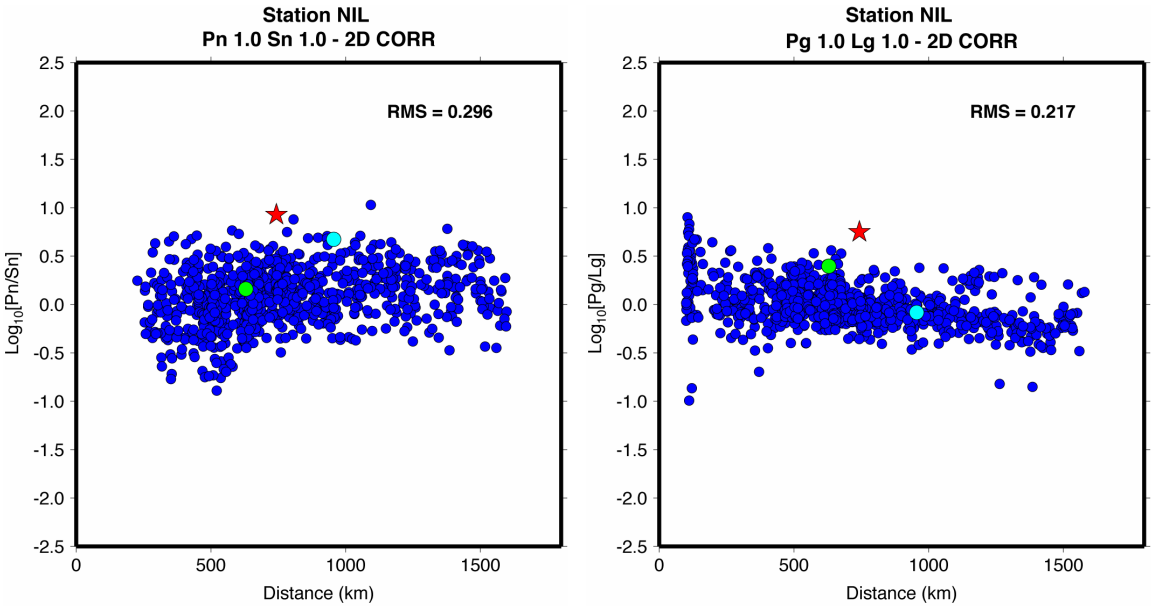

Figure 6. Pn/Sn and Pg/Lg discriminant at 1-2 Hz frequency recorded at station NIL showing data with attenuation corrections. In both panels, the three waveforms shown in Figure 1 are indicated by their corresponding color. Figure from Pasyanos and Walter (2009).

Since regional P/S discriminants generally work better at higher frequencies, we have also applied the attenuation model to higher-frequency discriminants. The path coverage for the upper mantle phases Pn and Sn is much better than crustal phases at high-frequencies, so we have used the Pn/Sn discriminant for the 4-6 Hz passband at station HASS in Saudi Arabia (Figure 7). Here, we see a similar reduction in the spread of the earthquake population, as well as an improvement in the discrimination of the 1998 Pakistani nuclear test.

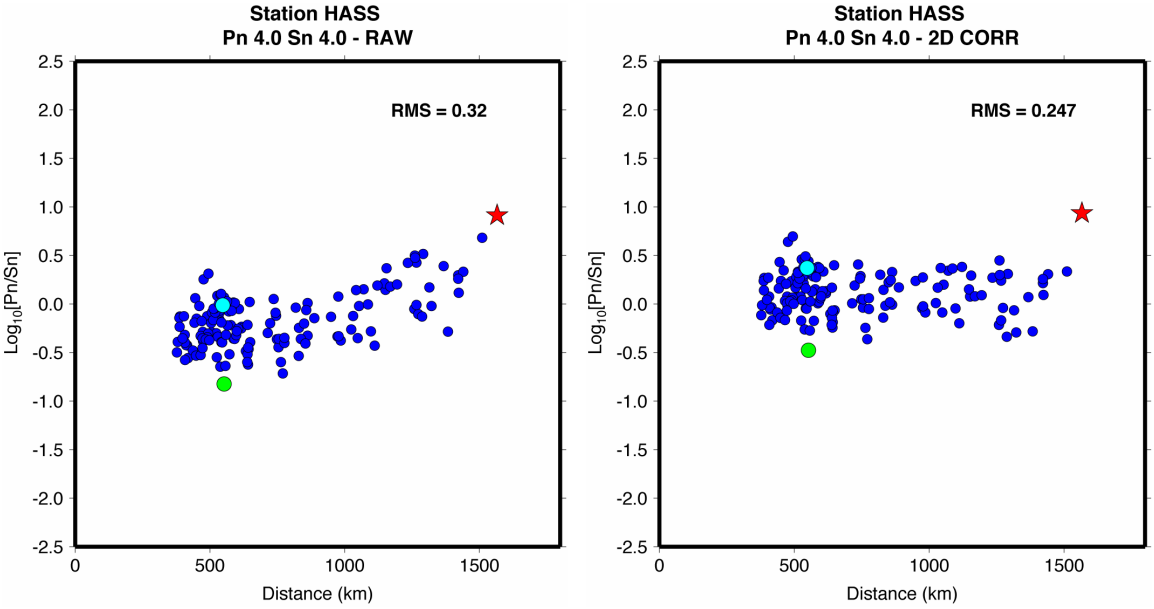

Figure 7. Pn/Lg discriminant at 4-6 Hz frequency recorded at station HASS showing raw data and data with attenuation corrections. In both panels, the red star corresponds to the 1998 Pakistani nuclear test and the green and blue circles are two earthquakes from the Zagros Mts.

Even with attenuation-based path corrections, there is still some variations in the P/S ratios as shown by the green and cyan circles in Figure 7 – two Zagros earthquakes which have very different P/S ratios. These unmodelled

amplitude variations can come from a number of possible sources, including small scale Q variations, variations in the source term (from seismic moment, apparent stress, depth, etc.), differences in geometrical spreading, earthquake mislocations, and multipathing, to name a few. We would like to explore the dataset to determine the major causes of the remaining variation.

CONCLUSIONS AND RECOMMENDATIONS

Attenuation tomography can capture the observed variability of regional phase amplitudes. The new attenuation tomography method that we have developed allows us to simultaneously invert for the amplitudes of regional phases Pn, Pg, Sn, and Lg. We have demonstrated that it is possible to use information about attenuation of the lithosphere to improve regional P/S discriminants. The new attenuation model has the potential to greatly improve earthquake-explosion discrimination in the Middle East and other tectonically complex regions. The challenge will come in calibrating attenuation structure at higher frequencies where the P/S discriminant appears to work better, but where data coverage for the tomographic model is sparser. Other challenges will be calibrating broad areas that include aseismic regions.

ACKNOWLEDGMENTS

We thank Stan Ruppert and Terri Hauk for maintaining the LLNL Seismic Research Database. We thank Doug Dodge and Mike Ganzberger for developing the RBAP code, which is used to make the regional amplitude measurements.

REFERENCES

Bird, P. (2003). An updated digital model of plate boundaries, *Geochem. Geophys. Geosyst*., 4, 1027, doi:10.1029/2001GC000252.

Camp, V. and M. Roobol (1992). Upwelling asthenosphere beneath western Arabia and its regional implications, *J. Geophys. Res.,* 97, 15,255-15,271.

Pasyanos, M.E. and W.R. Walter (2009). Improvements to regional explosion identification using attenuation models of the lithosphere, *Geophys. Res. Lett.,* in press, doi:10.1029/2009GL038505.

Pasyanos, M.E., E.M. Matzel, W.R. Walter, and A.J. Rodgers (2009a). Broad-band Lg attenuation modeling of the Middle East, *Geophys. J. Int.,* 177, 1166-1176, doi:10.1111/j.1365-246X.2009.04128.x

Pasyanos, M.E., W.R. Walter, and E.M. Matzel (2009b). A simultaneous multi-phase approach to determine P-wave and S-wave attenuation of the crust and upper mantle, in press, *Bull. Seism. Soc. Amer.*, 99-6.

Street, R.L., R. Herrmann, and O. Nuttli (1975). Spectral characteristics of the Lg wave generated by central United States earthquakes, *Geophys. J. R. Astron. Soc*., 41, 51-63.

Walter, W.R. and S.R. Taylor (2001). A revised magnitude and distance amplitude correction (MDAC2) procedure for regional seismic discriminants: theory and testing at NTS, Lawrence Livermore National Laboratory, UCRL-ID-146882, http://www.llnl.gov/tid/lof/documents/pdf/240563.pdf

Walter, W.R., M.E. Pasyanos, E. Matzel, R. Gok, J.J. Sweeney, S.R. Ford, and A.J. Rodgers (2008). Regional seismic amplitude modeling and tomography for earthquake-explosion discrimination, in *Proceedings of the 30th Monitoring Research Review: Ground-Based Nuclear Explosion Monitoring Technologies,* LA-UR-08-05261, pp. 702-711.

This work performed under the auspices of the U.S. Department of Energy by Lawrence Livermore National Laboratory under Contract DE-AC52-07NA27344.